Advances in Concrete Construction, *Vol. 10, No. 1* (*2020*) *81-92*
DOI: https://doi.org/10.12989/acc.2020.10.1.081

Assessment of flexural and splitting strength of steel fiber reinforced concrete using automated neural network search

Zhenhao Zhang[1], Suvash C. Paul[2], Biranchi Panda[3], Yuhao Huang[4], Ankit Garg[5], Yi Zhang[6], Akhil Garg[4] and Wengang Zhang*[7]

[1]*School of Civil Engineering, Changsha University of Science and Technology, 960 2nd Section of Wanjiali South Road, Changsha, Hunan, China*
[2]*Civil Engineering, School of Engineering, Monash University Malaysia, Jalan Lagoon Selatan, 47500 Bandar Sunway, Selangor Darul Ehsan, Malaysia*
[3]*Singapore Centre for 3D Printing, School of Mechanical & Aerospace Engineering, Nanyang Technological University, 50 Nanyang Avenue, Singapore*
[4]*Intelligent Manufacturing Key Laboratory of Ministry of Education, Shantou University, 243 Daxue Road, Jinping District, Shantou City, Guangdong Province, China*
[5]*Department of Civil and Environmental Engineering, Shantou University, 243 Daxue Road, Jinping District, Shantou City, Guangdong Province, China*
[6]*Leibniz Universität Hannover, 1 Welfengarten, Hannover, Germany*
[7]*School of Civil and Architectural Engineering, Shandong University of Technology, 266 Xincun West Road, Zhangdian District, Zibo City, Shandong Province, China*

(*Received July 12, 2018, Revised June 25, 2020, Accepted July 5, 2020*)

Abstract. Flexural and splitting strength behavior of conventional concrete can significantly be improved by incorporating the fibers in it. A significant number of research studies have been conducted on various types of fibers and their influence on the tensile capacity of concrete. However, as an important property, tensile capacity of fiber reinforced concrete (FRC) is not modelled properly. Therefore, this paper intends to formulate a model based on experiments that show the relationship between the fiber properties such as the aspect ratio (length/diameter), fiber content, compressive strength, flexural strength and splitting strength of FRC. For the purpose of modeling, various FRC mixes only with steel fiber are adopted from the existing research papers. Automated neural network search (ANS) is then developed and used to investigate the effect of input parameters such as fiber content, aspect ratio and compressive strength to the output parameters of flexural and splitting strength of FRC. It is found that the ANS model can be used to predict the flexural and splitting strength of FRC in a sensible precision.

Keywords: fiber aspect ratio; fiber content; compressive strength; flexural strength; splitting strength, FRC; ANS

1. Introduction

Since the 1980s, with the rapid development of computer and information technology, artificial intelligence has been gradually applied in various fields, and Artificial Neural Network (ANN) is one of the most widely used. ANNs provide a way to deal with complex and fuzzy problems with incomplete and inaccurate knowledge. ANNs are non-linear dynamic systems developed by simulating the biological neural structure system, and it can establish the implicit and complex relationship between input and output through training and learning, which is suitable to the problems difficult to solve by traditional calculation methods (Adeli 2001). Due to its strong nonlinearity, adaptability and fault tolerance, ANNs have been widely used in the field of civil engineering, such as material performance prediction, damage identification, bearing capacity analysis, optimal design, prediction of structural seismic response, construction management, etc. Adeli and Yeh (1989) published the first journal article on civil engineering applications of neural networks and applied perceptron to the design of steel beam with the length member, the unbraced length, the maximum bending moment, the maximum shear force and the ten times of bending coefficient as the inputs to predict whether the design of steel beam is acceptable. Stephens and Vanluchene (1994) trained a neural network model with three quantitative damage indexes as the inputs to assess the safety condition of earthquake-damaged structures. The results show that the neural network method is more reliable than the linear regression method. Based on a large number of test data, Buenfeld and Hassanein (1998) developed several ANNs predicting chloride profiles, chloride binding and carbonation depth to assist life prediction of concrete structures with steel corrosion. Georgy *et al*. (2005) applied neurofuzzy intelligent systems to predict the engineering performance in a construction project, and the neurofuzzy intelligent system combines ANNs and fuzzy control system, which offers the learning capabilities of ANNs while maintaining the flexibility in variable description of fuzzy-based modeling. Li *et al*. (2011) proposed a damage identification method that

*Corresponding author, Ph.D.
E-mail: ziwuzizwg@sdut.edu.cn

ISSN: 2287-5301 (Print), 2287-531X (Online)

compresses the pattern changes in frequency response function (FRFs) to a few principal components as the input of neural network model to estimate the structural damage. Yi *et al*. (2013) proposed a multi-stage structural damage diagnosis method based on the "energy-damage" theory, where the wavelet packet component energies are adopted as input into an improved back propagation neural network model. Gholizadeh (2015) combined a modified firefly algorithm and ANN to develop an efficient method for performance-based optimum seismic design of steel moment frames.

With the application of neural networks in the field of civil engineering, many researchers try to use ANNs to predict the mechanical properties of concrete. Kasperkiewicz *et al*. (1995) utilized ANNs for predicting strength properties of high-performance concrete with the inputs as six components, and the results suggest that the ANN can predict concrete performance effectively even with data complexity, incompleteness, and incoherence. Gupta *et al*. (2006) applied a neural network to predict concrete strength based on several parameters like concrete mix design, size and shape of specimen, curing technique and period, and environmental conditions, and a neural-expert system based on ANN was developed where the update of the knowledge can be used for neural-expert system enhancement. Saridemir (2009) developed an ANN to predict the compressive strength of concrete containing metakaolin and silica fume at different time points, and the results show that the compressive strength of the concrete can be predicted by ANN with tiny error rates. Duan *et al*. (2013) used ANN to predict the compressive strength of recycled aggregate concrete, where 14 inputs related to the materials of concrete are adopted. Ziolkowski and Niedostatkiewicz (2019) proposed the optimal ANN architecture to predict the compressive strength of the concrete resulting from a specific composition of concrete mix ingredients and translated the ANN into a mathematical equation that can be used in practical applications.

The application of ANNs in civil engineering has been introduced there, especially in the prediction of concrete performance, which indicates that ANNs can effectively predict the performance of various types of concrete. This study aims to develop a model that can predict the flexural strength and splitting strength of FRC. To achieve the goal of this study, a modeling tool automatic neural network search (ANS) is developed and used. It is noticed in the literature that, researchers have already made use of ANS to predict the capacity of FRC beams in shear (Paul *et al*. 2018). In fact, the principle of ANS has been widely used that find the optimum ANN by comparing the performance of different ANNs (Duan *et al*. 2013). In ANS, the relationships between input and output variables are generated by the data themselves. Also, ANS can tolerate relatively imprecise or incomplete tasks, approximate results, and even less vulnerable to outliers (Al-Saleh and Sundararaj 2011). For the inputs and outputs of ANS model, a total of 79 mix designs for FRC with steel hooked typed fibers were retrieved from the published papers and summarized for modeling. The detailed outcomes from the ANS model are discussed in the subsequent sections.

2. Properties of fiber reinforced concrete (FRC)

Various types of macro and micro synthesis and steel fibers are available on the market which can serve for the different purposes of concrete properties such as to control creep and shrinkage, increase the initial first cracking strength, preventing micro-cracks, etc. (Babafemi and Boshoff 2015, Paul and van Zijl 2016, Olivito and Zuccarello 2010). In the literature, many studies attempted to evaluate the enhancement of the flexural and tensile capacity of FRC associated with the types and contents of steel fibers (Lee *et al*. 2017, Alberti *et al*. 2017, Ganesan *et al*. 2017). The superiority of FRC has already been acknowledged by the researchers. Although, the overall performance of concrete improves when fibers are used, however, the dispersion of fiber and ease of handling also known as the workability of FRC is the challenging tasks. Typically, the workability of FRC reduces as the fiber volume increases. Also, the size and shape (straight or hooked) of fiber control the workability.

2.1 Assessment of fresh state of FRC properties

In order to characterize the fresh properties of FRC, typically slump-flow/slump cone, V-funnel and L-Box tests are performed. Generally, addition of fibers had more influence on the flow properties with significant reduction of the diameter of the patty. Using 0.33% steel fiber (l=35 mm, diameter=0.55 mm) in the mix, Alberti *et al*. (2017) observed about 13% lower slump-flow value and 25% higher time for V-funnel test in FRC than the control mix without any fiber. Similar behavior of FRC was also anticipated by other researchers (Nagananda *et al*. 2015, Shende *et al*. 2012, Yoo *et al*. 2015, Frazão *et al*. 2015). Ponikiewski *et al*. (2015) stated that slump-flow value reduces as the fiber volume increases. About 3% to 11% lower slump-flow was measured in FRC with low carbon crimped steel fiber (l=35 mm, width 2.6 mm) content 0.5% to 1.5%. For the same fiber volume, but different aspect ratios also influenced the flow behavior of FRC. Nagananda *et al*. (2015) reported about 5% to 7% lower slump value (slump cone test) with fiber volumes of 0.30% and 1.1% in FRC when the aspect ratio of the same fiber was increased from 65 to 80. The distribution of fibers in the matrix is influenced by the workability or vice versa. Addition of too long fibers tends to ball in the mix and create workability problems.

2.2 Hardened properties of FRC

Lee *et al*. (2017) studied the influence of volume fraction (0.25%, 0.375% and 0.50%) of steel fiber (hooked-end type) content in the flexural strength and crack mouth opening displacement (CMOD) in the different graded FRC. It was found that the first-cracking strength increases as the fiber volume increases in the mix. Similar behavior was also seen in the residual flexural strengths (strength after the first crack). Shende *et al*. (2012) investigated the compression and flexural strength behavior of FRC with 1%, 2% and 3% fiber volumes and 50, 60 and 67 fiber

aspect ratios. Both strengths were increased as the fiber volume increased. However, strengths were decreased for higher fiber aspect ratio. Compressive strength of FRC was reduced to about 4% and 6% when the fiber aspect ratio increased to 60 and 67 from 50. Likewise, with the aspect ratio of 50, increasing fiber volume from 1% to 3%, about 8% and 18% higher compressive and flexural strengths were found in FRC (Shende *et al*. 2012). Yoo *et al*. (2015) stated that increasing fiber volume in normal strength concrete can negatively influence the compressive strength. FRC specimens were made both for normal (below 50 MPa) and high strength (above 90 MPa) concrete with different fiber volumes. About 17% lower compressive strength was noticed in the normal strength FRC specimens with 2% fiber content when compared with reference concrete without any fiber in it. On the contrary, for the same fiber volume, about 7% higher compressive strength was noticed in high strength FRC specimens. This difference in strength can be explained by the crack initiation and air content in the normal and high strength FRC. Typically, in lower strength concrete, crack initiation starts early than in high strength concrete.

Like strength, the modulus of elasticity of FRC also marginally affects by the fiber volume and fiber aspect ratio. For both normal and high strength FRC, Yoo *et al*. (2015) reported that modulus of elasticity reduces as the fiber volume increases. The lower value of modulus of elasticity was attributed by the stress-strain curve of FRC during compression test. The slope of the stress-strain curve was found to be lower for increased fiber volume. In general, the deflection at the peak load was higher for higher fiber volume. It is due to fact that the fibers have superior crack-bridging capacity, and this leads to a higher load-carrying capacity after the first cracks appear (Marar *et al*. 2017, Shende *et al*. 2012, Yoo *et al*. 2015). Finally, inclusions of steel fibers in concrete contribute to the increase of residual strength in the post peak phase of the material, with a satisfactory effect in terms of its energy absorption capability (Frazão *et al*. 2015). Note that all the experimental results reported here are for 28 days.

2.3 Durability of FRC

Generally speaking for concrete structures, structural durability essentially unchanged during the first 10 years of service, but then begins to deteriorate apparently (Zhang *et al*. 2019, Zhang *et al*. 2020). Corrosion of steel bars inside concrete is considered to be most crucial for the durability of RC structures. However, it is reported in the literature that the steel fiber corrosion is less severe than the steel bars corrosion due to the large surface area to volume ratio. Smaller surface area of steel fibers can easily be covered by the rich lime film of binder paste than the large diameter of conventional steel bars (Frazão *et al*. 2015, Woo *et al*. 2014). Nonetheless, micro-spalling of concrete and reduction of sectional area of steel fibers can be seen due to the corrosion, which is a major fact for durability of FRC elements (Fritih *et al*. 2013).

Frazao *et al*. (2015) reported that adding 2.5% fibers (l=35 mm, diameter is 0.50 mm) in the mix increased slightly higher capillary water absorption of self-consolidating concrete (SCC) than the control mix of SSC. It was concluded that the capillary pore size in the matrix did not substantially alter due to addition of fibers. Therefore, no significant difference in the water absorption noticed in SSC with and without fibers. This phenomenon was also proved by Yehia *et al*. (2016) when rapid chloride penetration test performed in FRC. Though chloride penetration was slightly higher in FRC, however, high density of matrix did not show any significant difference in chloride penetration in FRC and control specimens. To end, research on durability of steel fibers is still scarce, especially corrosion, where it is still not clear whether corrosion of fibers really contributes to the cracking and spalling of cover concrete. More research is required in this field to come up with a solid conclusion.

From the discussion above, it is postulated that the selection of proper fiber types, size, volume and mix compositions are important for mechanical and durability behavior of FRC. The character of FRC also changes with varying concretes, fiber materials, geometries, distribution, orientation and densities. Therefore, a proper understating is required for the properties of fiber and the performance of FRC. In this regard, this study aims to develop a model that can predict the relationship between the fiber properties like aspect ratio (length/diameter), fiber content, compressive strength, flexural strength and splitting strength of FRC. Note that the aspect ratio of fiber measure the slenderness ratio of individual fiber typically computed as length divided by the equivalent diameter and typically aspect ratio varies from 30 to 150, and the amount of fibers added to a concrete mix is measured as a percentage of the total volume of the composite, and typically ranges from 0.1 to 3%.

Table 1 Sample of data collection for ANS modelling

Authors	Input			Output	
	Fiber content (%)	Aspect ratio (l/d)	Comp. Strength (MPa)	Flexural strength (MPa)	Splitting strength (MPa)
Afroughsabet and Ozbakkaloglu (2015)	0.25	80	92.30	8.93	6.05
	0.50	80	93.80	9.97	6.41
	0.75	80	95.00	10.61	7.29
	1.00	80	98.70	12.58	8.17
Shende *et al*. (2012)	1.00	50	52.00	8.80	3.30
	2.00	50	53.33	9.47	3.92
	3.00	50	56.30	10.40	4.34
Söylev and Özturan (2013)	0.50	64	38.00	4.30	3.60
Fatima and Varghese (2014)	0.25	50	40.83	4.32	3.55
	0.50	50	46.73	5.20	3.96
	0.75	50	50.63	5.68	4.31
Sarbini *et al*. (2011)	0.25	80	40.39	3.78	2.78
	0.50	80	40.79	3.91	3.09
	0.75	80	37.63	4.57	4.30
	1.00	80	38.07	5.79	5.21
	1.25	80	46.68	6.81	6.41
	1.50	80	47.01	8.08	6.14
	1.75	80	46.47	7.12	7.05

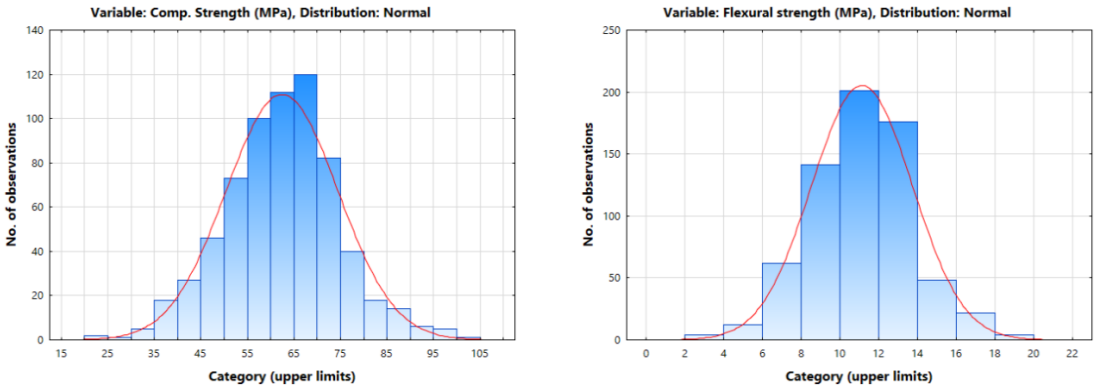

(a) Compressive strength

(b) Flexural strength

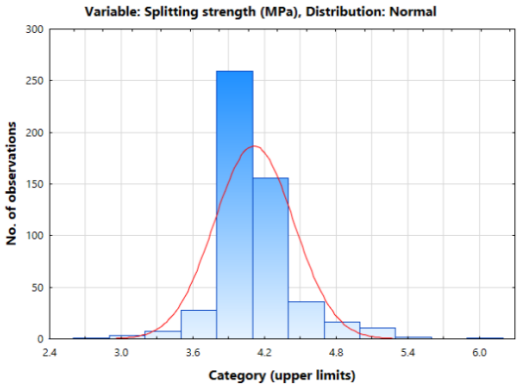

(c) Splitting strength

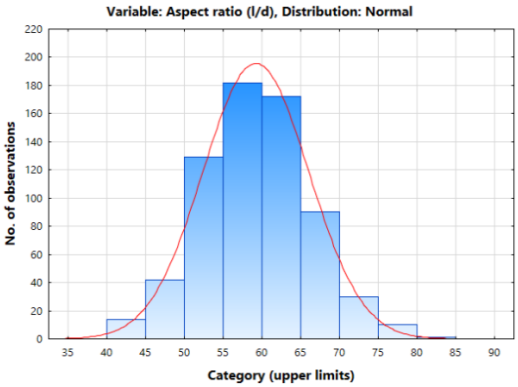

(d) Aspect ratio

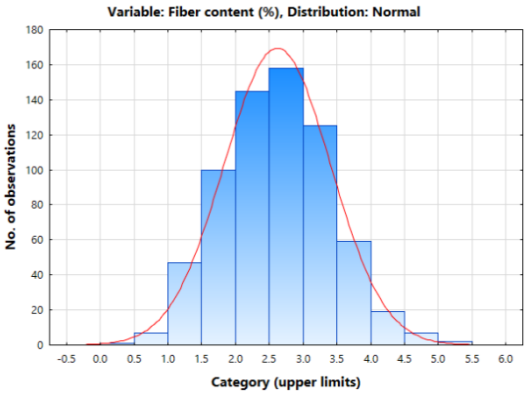

(e) Fiber content

Fig. 1 Normal distributions of input and output data used for ANS model

3. Data preparation and automatic neural network system (ANS)

3.1 Data collection for ANS model

For modeling ANS of FRC strength, a total of 79 different mix designs was selected (Afroughsabet and Ozbakkaloglu 2015, Olivito and Zuccarello 2010, Lee *et al*. 2017, Nagananda *et al*. 2015, Shende *et al*. 2012, Yoo *et al*. 2015, Söylev and Özturan 2013, Fathima and Varghese 2014, Vairagade and Kene 2013, Sarbini *et al*. 2011) to train and check the reliability of strength data. All the mix designs were collected from the FRC where only hooked steel fibers were used. Cubes and prisms (beam shape) specimens were made and tested at 28 days for determining the ultimate compressive, flexural and splitting strength of FRC. A sample of data collections are shown in Table 1. A total of three parameters were used as input for ANS model as they are also defined in Table 1. The 28 day flexural and splitting strengths were the output value considered in the paper. Taking into account that different researchers used different mix compositions for FRC, therefore, the compressive strength was considered as an input parameter for the ANS model. The following sections discussed the ANS model preparation and outcome in detail.

Normal distributions of input and output data are shown in Fig. 1. It can be seen that except for splitting strength shown in Fig. 1(c), the shape of the normal distributions shows perfect symmetry of the data. The center of a normal distribution is located at its peak, and 50% of the data lies

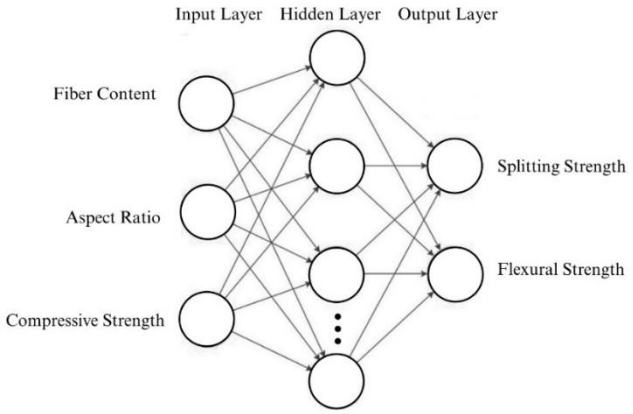

Fig. 2 Illustration of the ANS

above the mean, while 50% lies below. Normal distributions are often represented in standard scores, or Z scores. Z scores are numbers that tell us the distance between an actual score and the mean in terms of standard deviations. For any modeling, proper data collection and distribution of data are very important. Therefore, it is necessary to have the normal distribution in the data.

3.2 ANS model

ANS has the same principle as ANNs, but ANS automates the selection of the number of units in the hidden layer, the selection of the activation functions and the selection of the training algorithm. Using too few units in the hidden layer will result in underfitting. On the contrary, using too many units may lead to overfitting. Obviously, it is extremely important to choose a suitable number of units in the hidden layer. There is no systematic way of determining the optimal number of hidden units and the best activation function, and the most common way to optimize models is by educated trial and error (Buenfeld and Hassanein 1998). In ANS, by setting the optional network types and activation functions, as well as the maximum and minimum number of hidden units, and utilizing the data to train and detect different ANNs to find the optimal ANN by comparing the correlation coefficient automatically.

There are three types of units in an ANN: input unit, output unit and hidden unit. The input units receive the external input signal, the hidden units and the output units process the signal received from the former layer, and the final results are output by the output units. The connection between each two units represents the weight of the signal passing through the connection, which reflects the connection strength between the two units. There is an activation function in each hidden unit and output unit to introduce nonlinear factors into the neural network. Through the activation functions, the neural network can fit various curves. Therefore, the output of the network depends on the structure of network, weight values between the units, and activation functions. Before training a neural network, the structure of the network and the activation functions of the units have been determined, so the learning process of the neural network is the process of changing the weight matrix (Haykin 1999). In this study, ANS consists of the three layers, the input layer comprising of the three design variables (fiber content, aspect ratio and compressive strength), the hidden layer comprising of the unknown number of neurons and the output layer comprising of the two outputs (splitting strength and flexural strength)as shown in Fig. 2.

There are two optional network types in ANS which are Multi-layer Perceptron (MLP) and Radial Basis Functions Neural Networks (RBF). Both MLP and PBF are non-linear feedforward neural networks.

MLP is generally composed of one input layer, one output layer and one or several hidden layers. There are connections between the units of two adjacent layers, but not between the units of the same layer. The outputs of the former layer are the inputs of the next layer, and each layer only receives the output signal of the former layer. Two important characteristics of MLP are its non- linear processing units which have a non-linear activation function that must be smooth (the logistic function and the hyperbolic tangent are the most widely used) and that any unit of a given layer feeds all the units of the next layer (Memarian and Balasundram 2012). The two common activation functions used in MLP are Logistic and Tanh are shown as follows

$$logistic(x) = \frac{1}{1+e^{-x}} \tag{1}$$

$$tanh(x) = \frac{e^{x}-e^{-x}}{e^{x}+e^{-x}} \tag{2}$$

and MLP with a single hidden layer can be expressed as

$$y_k = f(\sum_{j=1}^{n} w_{jk}^{(2)} a_j + \theta_k^{(2)}) \tag{3}$$

$$a_j = g(\sum_{i=1}^{m} w_{ij} x_i + \theta_j) \tag{4}$$

where y_k is the output of the k-th unit in the output layer; $f(g)$ is the activation function of output layer; $w_{jk}^{(2)}$ is the weight from the j-th unit in hidden layer to the k-th unit in output layer; $\theta_k^{(2)}$ is the bais of the j-th unit in hidden layer; a_j is the output of the j-th unit in hidden layer; x_i is the input of the i-th unit in input layer; $g(g)$ is the activation function of hidden layer; w_{ij} is the weight from the i-th unit in input layer to the j-th unit in hidden layer; θ_j is the bais of the j-th unit in hidden layer; m and n are the number of units in the input layer and hidden layer respectively. The illustration of MLP network with a single hidden layer is shown in Fig. 3.

RBF is a three-layer neural network composed of one input layer, one hidden layer and one output layer. Compared with MLP, the hidden units of RBF take the Euclidean distance between the input vector and the center vector as the independent variable, and use radial basis functions (usually as Gaussian function) as the activation functions without connection weight. The transformation from input layer to hidden layer is non-linear, but the transformation from the hidden layer to the output layer is

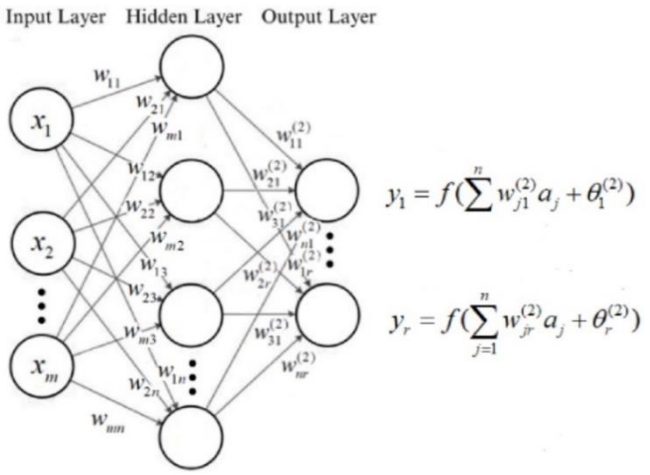

Fig. 3 Illustration of MLP with single hidden layer

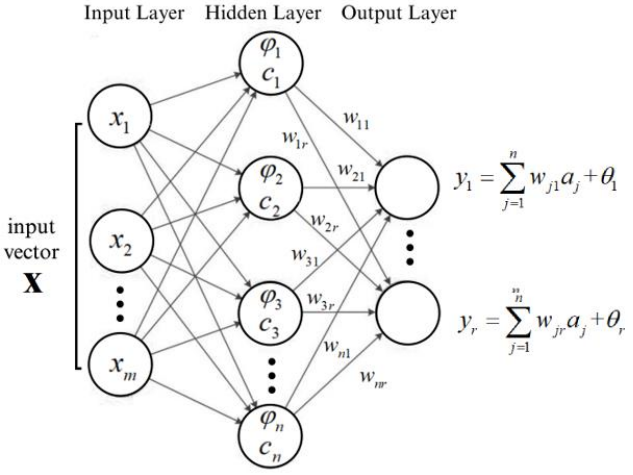

Fig. 4 Illustration of RBF

linear (Chen *et al*. 1991). According to Cover's theorem, the data that can't be divided in low-dimension space may be divided in high-dimension space, which reveals that the function of the hidden layer of RBF network is to map the input of low-dimensional space to a high-dimensional space through nonlinear functions, and carry out curve fitting in the high-dimensional space. It is equivalent to finding a surface that can best fit the training data in an implicit high-dimensional space. The output layer then implements a linear combiner on this new space (Chen *et al*. 1991).

RBF network with Gaussian function as activation function can be expressed as follows

$$y_k = \sum_{j=1}^{n} w_{jk} a_j + \theta_k \tag{5}$$

$$a_j = \varphi_j(\mathbf{x}) = exp(-\frac{\left\|\mathbf{x} - \mathbf{c}_j\right\|^2}{2\sigma^2}) \tag{6}$$

where y_k is the output of the k-th unit in the output layer; w_{jk} is the weight from the j-th unit in hidden layer to the kth unit in output layer; a_j is the output of the j-th unit in hidden layer; θ_k is the bais of the k-th unit in output layer; $\mathbf{x}$ is input vector; φ_j is the activation function of the j-th hidden unit; $\mathbf{c}_j$ is the RBF center of the j-th hidden unit; $\|\mathbf{x}-\mathbf{c}_j\|$ is the Euclidean distance between the sample and the RBF center; σ is known as wide value, usually as a constant; The illustration of RBF network is shown in Fig. 4.

The data collected are divided into training and testing in the standard range of 8:2 ratios and fed into the framework of ANS. ANS is used for formulating the neural networks with various configurations and settings while requiring nominal specifications. It forms a number of network models with algorithmic combinations (Garg *et al*. 2019), and tries to find the optimal ANN by comparing the correlation coefficient. The experimental design on the following settings was performed.

Training: 80% testing:20% validation:0%
Network settings
1. Multi-Layer Perceptron (MLP)
min hidden units 3
max hidden units 100

2. Radial-basis function (RBF)
min hidden units 12
max hidden units 50

Networks to train: 2000
Networks to retain: 10

MLP Activation Functions (for both hidden neurons and output neurons):
Identity, Logistic, Tanh, Exponential, Sine

Weight decay (for both hidden layers and output layers):
Min 0.0001
Max 0.001

Fixed seed for network initialization
seed value 1000

The work conducts quantitative analysis on each neural network to choose the settings that give the best performance of ANS models on two outputs. The best design RBF 3-13-2 was selected based on the minimum correlation coefficient (R) on the training data.

4. Results and discussion

Tensile strength is one of the most important characteristics of FRC where fibers play an important role in reaching certain load-carrying capacity after the first crack appears to the matrix, depending on fibers dispersion, alignments and embedded length (Holschemacher *et al*. 2010). A strong mechanical interlocking force in FRC specimens can be expected due to inclusion of fibers which hold the matrix stronger and concrete remains intact even after failure loading, whereas conventional concrete (without any fibers) after failure splits into large pieces (Tanoli *et al*. 2014).

For modeling part, after the network has been trained well. The parametric studies are carried out focusing on the effect of a particular variable and compared with similar test results to study if the ANS is able to predict the

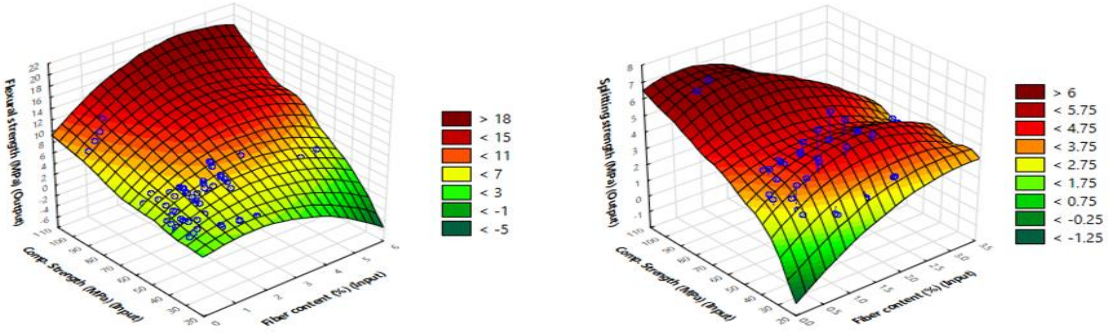

(a) Flexural strength (b) Splitting strength

Fig. 5 Influence of incorporating compressive strength and fiber content on flexural and splitting strength of FRC at 28 days

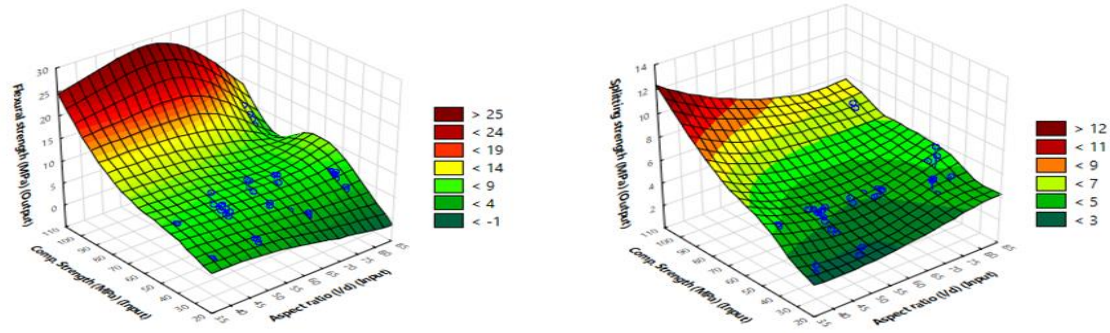

(a) Flexural strength (b) Splitting strength

Fig. 6 Influence of incorporating compressive strength and aspect ratio on flexural and splitting strength of FRC at 28 days

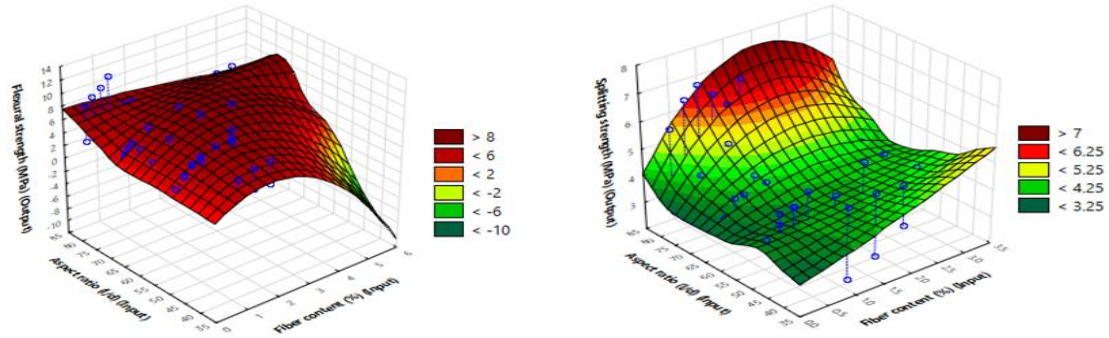

(a) Flexural strength (b) Splitting strength

Fig. 7 Influence of incorporating aspect ratio and fiber content on flexural and splitting strength of FRC at 28 days

experimental trend. These studies are carried out by simply varying one input parameter and keeping the others constant. This section describes the relationship between the input and output parameters found in ANS.

4.1 Relationship between fiber properties and strength of FRC

Crack propagations due to internal stress of concrete can be protected by the shear transferability of fiber. Based on geometry and content, fibers bear some stress that occurs in the cement matrix themselves and transfer other portion of stress to the stable cement matrix (Yazici *et al*. 2007). Thus, the relative strength capacity of FRC continues even after the crack appears to the matrix. The influence of incorporating compressive strength, fiber content and fiber aspect ratio on flexural and splitting strength of FRC is shown in Figs. 5-7. The model data shows that the flexural and splitting strength of FRC are not only related to its compressive strength, it also influenced by the fiber content and fiber aspect ratio. Fig. 5(a) shows that as the compressive strength and fiber content increase, flexural strength of FRC also increases. However, this phenomenon is partially valid for splitting strength as it is illustrated in Fig. 5(b). Although, splitting strength increases with the increase of compressive strength, but it can reduce when fiber volume reaches more than 2%. Similarly in Figs. 6(a)-(b), it is shown that as the fiber aspect ratio increases, both flexural and splitting strength reduce. Figs. 7(a)-(b) show the influence of fiber content and fiber aspect ratio on both flexural and splitting strength of FRC. It can be seen that fiber content is more dominant parameter for FRC strength

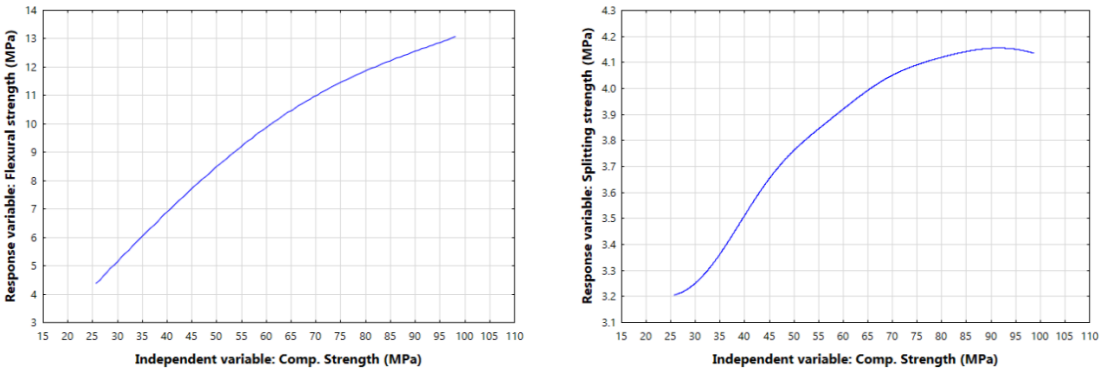

(a) Flexural strength (b) Splitting strength

Fig. 8 Effect of compressive strength on flexural and splitting strength of FRC

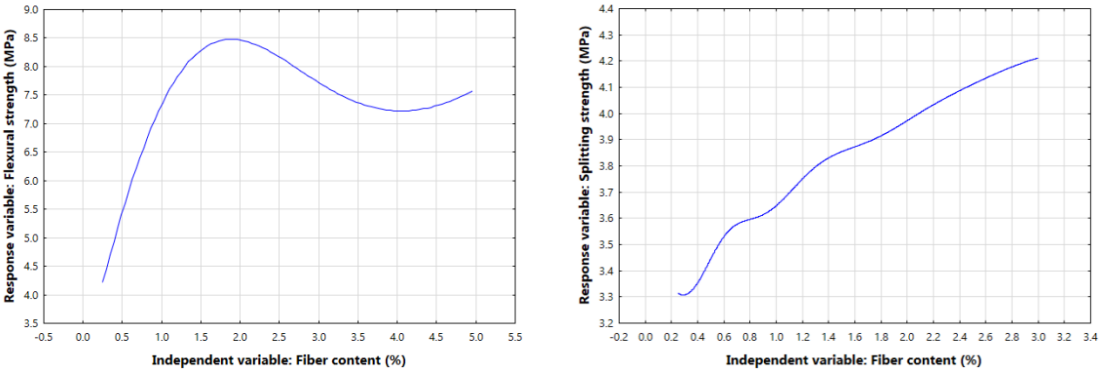

(a) Flexural strength (b) Splitting strength

Fig. 9 Effect of fiber content on flexural and splitting strength of FRC

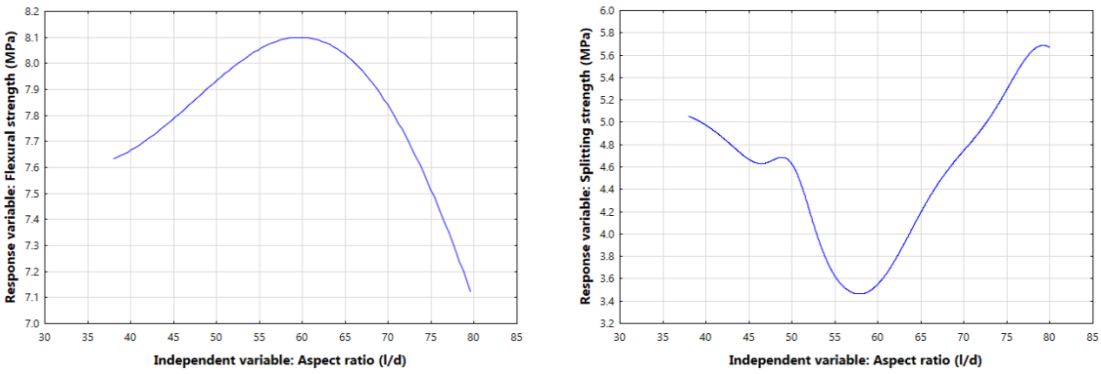

(a) Flexural strength (b) Splitting strength

Fig. 10 Effect of aspect ratio on flexural and splitting strength of FRC at 28 days

than the fiber aspect ratio. Too much fiber content creates weak interface bonding between the matrix and fibers due to possible congestions of fibers which create a barrier for binder paste to cover the total fiber surface. Therefore, the fiber and matrix interface adhesion strength reduce significantly. Higher fiber content may also lead to higher porosity in the matrix leading to lower strength.

The relationship between the independent variables of input and output parameters are shown in Figs. 8-10. The flexural and splitting strength of FRC increases exponentially with the increase of compressive strength as shown in Figs. 8(a)-(b). The effect of fiber content on FRC strengths also studied as shown in Figs. 9(a)-(b). Typically, higher modulus of elasticity of steel fibers in the matrix (concrete or mortar binder) helps to carry the load by increasing the tensile strength of the material. Increase in the aspect ratio of the fiber usually segments the flexural and splitting strengths as shown in Figs. 10(a)-(b). It is clear from Figs. 10(a)-(b) that higher aspect ratio (60 onwards) negatively influence on flexural strength.

4.2 Sensitivity analysis

Figs. 11(a)-(b) show the results of the sensitivity analysis measuring the amount of impact of inputs parameters on two response characteristics. This is done by

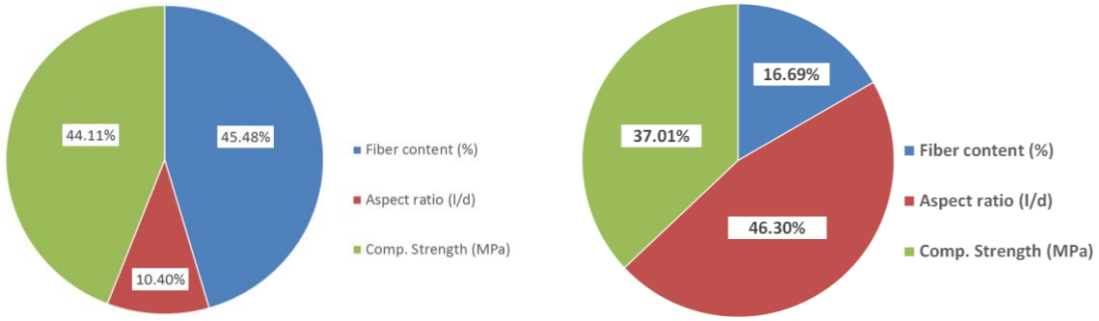

(a) Flexural strength (b) Splitting strength

Fig. 11 Sensitivity analysis of fiber content, aspect ratio and compressive strength on flexural and (b) splitting strength of FRC

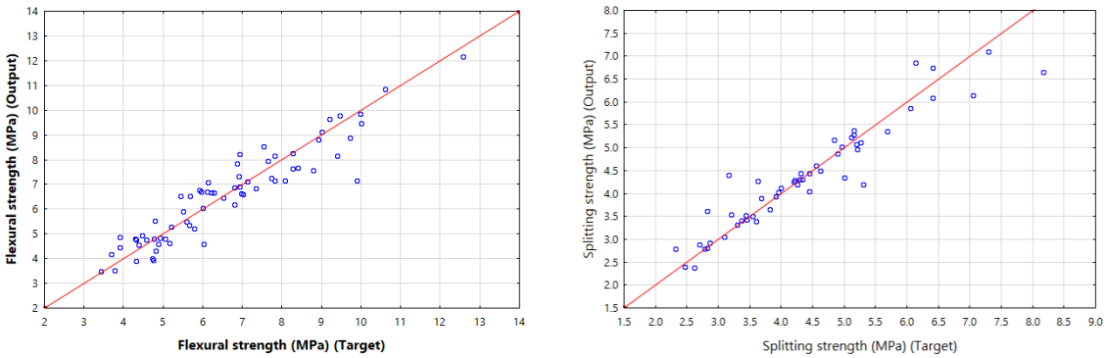

(a) Flexural strength (b) Splitting strength

Fig. 12 Performance of model on training and testing data of flexural and splitting strength

finding the maximum and minimum of two response characteristics from 2-D plots (Figs. 8-10) and counting the number of peaks of two response characteristics from 3-D plots (Figs. 6-8). It is found that, in flexural strength, fiber content and compressive strength contributed about 45% and 44%, respectively (see Fig. 11(a)). However, in splitting strength, fiber content and compressive strength contributed only about 17% and 37%. Interestingly, fiber content has less contribution to the splitting strength than in flexural strength. In splitting strength, fiber aspect ratio has more contribution than two other parameters. This interpretation from the sensitivity analysis is also in line with the findings from the parametric analysis as reported in Figs. 5-10. Thus, based on this analysis appropriate values of input parameters can be selected that can result in higher flexural and splitting strength of FRC.

From the discussion above and the research outcome shown in Figs. 5-10, it can be said that the results obtained using ANS model follow the experimental and real trends. This is further proved in Figs. 12(a)-(b) where target flexural and splitting strengths (these are obtained from experiments) and ANS model output depth follows a linear relationship. The prediction lies above or below of target line (the line where experimental and predicted value is equal). Prediction is considered to be better when the data points lie nearer to the diagonal line and this is related to the training of the data. However, in both cases, less scatter in the data points are obtained which confirms the efficiency of ANS as a predictor of FRC flexural and splitting strength.

Table 2 Optimum set of input values for maximum flexural strength and maximum splitting strength

Fiber content (%)	Aspect ratio (l/d)	Compressive strength (MPa)	Flexural strength (MPa)
3.57	47.64	98.70	19.69
Fiber content (%)	Aspect ratio (l/d)	Compressive strength (MPa)	Splitting strength (MPa)
1.50	79.66	46.46	6.87

4.3 Optimization results of the ANS model RBF 3-13-2

RBF 3-13-2 is optimized using the non-dominated sorted genetic algorithm-Ⅱ (NSGA-Ⅱ) combined with the simplex search algorithm to avoid any convergence in local minima. The iteration number (3000) is fixed to obtain the optimized value of flexural and splitting strengths of 19.69 MPa and 6.87 MPa. Figs. 13(a)-(b) show the desire value of flexural strength of concrete achieved is 19.69 MPa for iteration number 60 and 6.87 MPa splitting strength for the iteration number 68. The optimum value of the inputs required for achieving the desired strength is shown in Table 2.

5. Conclusions

This work attempts to solve the research problem on investigating the fiber properties (aspect ratio, fiber content and compressive strength) on the flexural and splitting

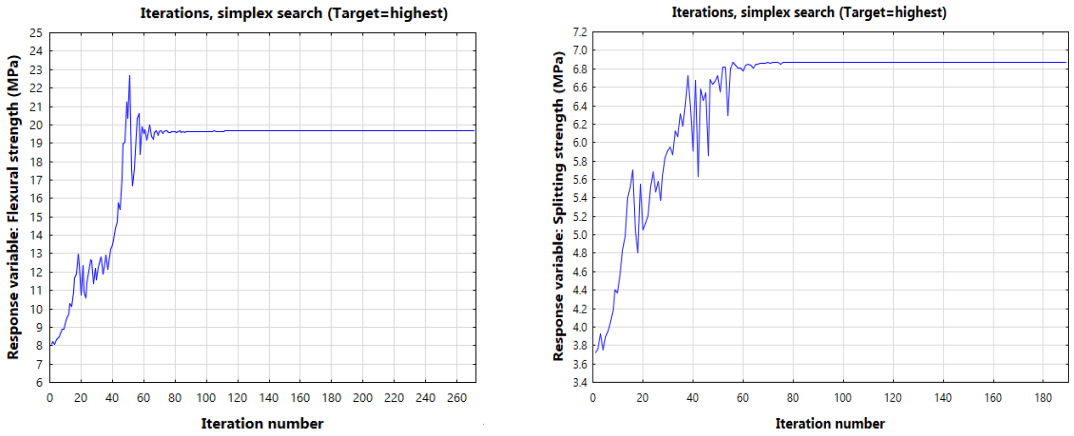

(a) Flexural strength (b) Splitting strength

Fig. 13 Plot showing convergence of desire value of highest of flexural and splitting strength

strength of concrete. Experiments are performed and the automated neural networks search (ANS) model is developed and optimized to determine the relationships (between the fiber properties and strength of fiber reinforced concrete (FRC)) and the optimum value of fiber content. From the outcome of the research, flexural and splitting strengths of FRC can be predicted from its compressive strength, fiber content and aspect ratio at a reasonable accuracy. However, the performance of ANS can further be improved with more parameters in future studies. It may be interesting to know whether the other parameters such as type of binders, aggregates properties, addition of admixtures, etc. can be modeled by ANS. Also, sufficient number of data should be considered for ANS to be able to model in an accurate manner. Further research should be undertaken to improve the ANS generalization ability for multiple variables.

The following conclusions and recommendations can be drawn from the outcome of this research:

- Artificial neural network search has fairly high accuracy on predicting the flexural and splitting strengths of FRC.
- Flexural and splitting strength increases with the increase of compressive strength and fiber content of the FRC matrix.
- Higher fiber aspect ratio (above 60) has both positive and negative influence on FRC strength. Flexural strength of FRC decreases when aspect ratio is above 60. However, splitting strength found to be increased for aspect ratio more than 60.
- Fiber content and compressive strength have much more influence in flexural strength than fiber aspect ratio. Aspect ratio and compressive strength have more influence in splitting strength than fiber content.
- The performance of the neural network search model is still to be improved by considering more parameters in the further research.

References

Adeli, H. (2001), "Neural networks in civil engineering: 1989-2000", *Comput. Aid. Civil Infrastr. Eng.*, **16**(2), 126-142. https://doi.org /10.1111/0885-9507.00219.

Adeli, H. and Yeh, C. (1989) "Perceptron learning in engineering design", *Comput. Aid. Civil Infrastr. Eng.*, **4**(4), 247-256. https://doi.org/10.1111/j.1467-8667.1989.tb00026.x.

Afroughsabet, V. and Ozbakkaloglu, T. (2015), "Mechanical and durability properties of high-strength concrete containing steel and polypropylene fibers", *Constr. Build. Mater.*, **94**, 73-82. https://doi.org/10.1016/j.conbuildmat.2015.06.051.

Al-Saleh, M.H. and Sundararaj, U. (2011), "Review of the mechanical properties of carbon nanofiber/polymer composites", *Compos. Part A: Appl. Sci. Manuf.*, **42**(12), 2126-2142. https://doi.org/10.1016/j.compositesa.2011.08.005.

Al-Taan, S.A., Al-Rifaie, W.N. and Al-Neimee, K.A. (2016), "Properties of fresh and hardened high strength steel fibers reinforced self-compacted concrete", *Proceedings of the 4th International Conference on Sustainable Construction Materials and Technologies*, Las Vegas, USA,. August.

Alberti, M.G., Enfedaque, A. and Gálvez, J.C. (2017), "Fibre reinforced concrete with a combination of polyolefin and steel-hooked fibres", *Compos. Struct.*, **171**, 317-325. https://doi.org/10.1016/j.compstruct.2017.03.033.

Babafemi, A.J. and Boshoff, W.P. (2015), "Tensile creep of macro-synthetic fibre reinforced concrete (MSFRC) under uni-axial tensile loading", *Cement Concrete Compos.*, **55**, 62-69. https://doi.org/10.1016/j.cemconcomp.2014.08.002.

Buenfeld, N.R. and Hassanein, N.M. (1998), "Predicting the life of concrete structures using neural networks", *Proc. Inst. Civil Eng. Struct. Build.*, **128**(1), 38-48. https://doi.org/10.1680/istbu.1998.30033.

Duan, Z.H., Kou, S.C. and Poon, C.S. (2013), "Prediction of compressive strength of recycled aggregate concrete using artificial neural networks", *Constr. Build. Mater.*, **40**, 1200-1206. https://doi.org/10.1016/j.conbuildmat.2012.04.063.

Fathima, A. and Varghese, S. (2014), "Behavioural study of steel fiber and polypropylene fiber reinforced concrete", *Int. J. Res. Eng. Technol.*, **2**(10), 17-24. https://doi.org/10.4028/www.scientific.net/KEM.708.59.

Frazão, C., Camões, A., Barros, J. and Gonçalves, D. (2015), "Durability of steel fiber reinforced self-compacting concrete", *Constr. Build. Mater.*, **80**, 155-166. https://doi.org/10.1016/j.conbuildmat.2015.01.061.

Fritih, Y., Vidal, T., Turatsinze, A. and Pons, G. (2013), "Flexural and shear behavior of steel fiber reinforced SCC beams", *KSCE J. Civil Eng.*, **17**(6), 1383-1393. https://doi.org/10.1007/s12205-013-1115-1.

Ganesan, N., Indira, P.V. and Irshad, P. (2017), "RCC frames with

ferrocement and fiber reinforced concrete infill panels under reverse cyclic loading", *Adv. Concrete Constr.*, **5**(3), 257-270. https://doi.org/10.12989/acc.2017.5.3.257.

Garg, A., Ruhatiya, C., Cui, X., Peng, X., Bhalerao, Y. and Gao, L. (2019), "A novel approach for enhancing thermal performance of battery modules based on finite element modelling and predictive model-ling mechanism", *J. Electrochem. Energy Convers. Storage*, **17**(2), 021103. https://doi.org/10.1115/1.4045194.

Georgy, M.E., Chang, L. and Zhang, L. (2005), "Prediction of engineering performance: a neurofuzzy approach", *J. Constr. Eng. Manage*., ASCE, **131**(5), 548-557. https://doi.org/10.1061/(ASCE)0733-9364(2005)131:5(548).

Gholizadeh, S. (2015), "Performance-based optimum seismic design of steel structures by a modified firefly algorithm and a new neural network", *Adv. Eng. Softw.*, **81**, 50-65. https://doi.org/10.1016/j.advengsoft.2014.11.003.

Gupta, R., Kewalramani, M.A. and Goel, A. (2006), "Prediction of concrete strength using neural-expert system", *J. Mater. Civil Eng.*, **18**(3), 462-466. https://doi.org/10.1061/(ASCE)0899-1561(2006)18:3(462).

Haykin, S. (1999), *Neural Networks: A Comprehensive Foundation*, 2nd Edition, Prentice Hall, New York, NY, USA.

Holschemacher, K., Mueller, T. and Ribakov, Y. (2010), "Effect of steel fibers on mechanical properties of high-strength concrete", *Mater. Des.*, **31**(5), 2604-2615. https://doi.org/10.1016/j.matdes.2009.11.025.

Kasperkiewicz, J., Racz, J.W. and Dubrawski, A. (1995), "HPC strength prediction using artificial neural network", *J. Comput. Civil Eng.*, **9**(4), 279-284. https://doi.org/10.1061/(ASCE)0887-3801(1995)9:4(279).

Lee, J.H. (2017), "Influence of concrete strength combined with fiber content in the residual flexural strengths of fiber reinforced concrete", *Compos. Struct.*, **168**, 216-225. https://doi.org/10.1016/j.compstruct.2017.01.052.

Lee, J.H., Cho, B. and Choi, E. (2017), "Flexural capacity of fiber reinforced concrete with a consideration of concrete strength and fiber content", *Constr. Build. Mater.*, **138**, 222-231. https://doi.org/10.1016/j.conbuildmat.2017.01.096.

Li, J., Dackermann, U., Xu, Y. and Samali, B. (2011), "Damage identification in civil engineering structures utilizing PCA-compressed residual frequency response functions and neural network ensembles", *Struct. Control Hlth. Monit.*, **18**(2), 207-226. https://doi.org/10.1002/stc.369.

Marar, K., Eren, O. and Roughani, H. (2017), "The influence of amount and aspect ratio of fibers on shear behaviour of steel fiber reinforced concrete", *KSCE J. Civil Eng.*, **21**(4), 1393-1399. https://doi.org/10.1007/s12205-016-0787-2.

Memarian, H. and Balasundram, S.K. (2012), "Comparison between multi-layer perceptron and radial basis function networks for sediment load estimation in a tropical watershed", *J. Water Res. Protect.*, **4**(10), 870-876. http://dx.doi.org/10.4236/iwarp.2012.410102.

Nagananda, V., Dattatreya, J.K. and Suresh, S. (2015), "Study on compressive behavior of steel fiber reinforced concrete", *J. Civil Eng. Environ. Technol.*, **2**(11), 37-40. https://doi.org/10.1061/(ASCE)MT.1943-5533.0000372.

Olivito, R.S. and Zuccarello, F.A. (2010), "An experimental study on the tensile strength of steel fiber reinforced concrete", *Compos. Part B: Eng.*, **41**(3), 246-255. https://doi.org/10.1016/j.compositesb.2009.12.003.

Panda, B., Paul, S.C. and Tan, M.J. (2017), "Anisotropic mechanical performance of 3D printed fiber reinforced sustainable construction material", *Mater. Lett.*, **209**, 146-149. https://doi.org/10.1016/j.matlet.2017.07.123.

Paul, S.C. and van Zijl, G.P.A.G. (2016), "Chloride-induced corrosion modelling of cracked reinforced SHCC", *Arch. Civil Mech. Eng.*, **16**(4), 734-742. https://doi.org/10.1016/j.acme.2016.04.016.

Paul, S.C., Panda, B. and Garg, A. (2018), "A novel approach in modelling of concrete made with recycled aggregates", *Measure.*, **115**, 64-72. https://doi.org/10.1016/j.measurement.2017.10.031.

Perera, R., Barchín, M., Arteaga, A. and Diego, A.D. (2010), "Prediction of the ultimate strength of reinforced concrete beams FRP-strengthened in shear using neural networks", *Compos. Part B: Eng.*, **41**(4), 287-298. https://doi.org/10.1016/j.compositesb.2010.03.003.

Ponikiewski, T., Gołaszewski, J., Rudzki, M. and Bugdol, M. (2015), "Determination of steel fibres distribution in self-compacting concrete beams using X-ray computed tomography", *Arch. Civil Mech. Eng.*, **15**(2), 558-568. https://doi.org/10.1016/j.acme.2014.08.008.

Sarbini, N.N., Ibrahim, I.S. and Saim, A.A. (2011), "Enhancement on strength properties of steel fibre reinforced concrete", *Proceedings of the 3rd European Asian Civil Engineering Forum*, Yogyakarta, Indonesia, September.

Saridemir, M. (2009), "Prediction of compressive strength of concretes containing metakaolin and silica fume by artificial neural networks", *Adv. Eng. Softw.*, **40**(5), 350-355. https://doi.org/10.1016/j.advengsoft.2008.05.002.

Söylev, T.A. and Özturan, T. (2013), "Strength and fracture toughness of fiber reinforced concrete", *Proceedings of 2nd International Conference on Smart Monitoring, Assessment and Rehabilitations of Civil Structures*, Istanbul, Turkey, September.

Stephens, J. and Vanluchene, R.D. (1994), "Integrated assessment of seismic damage in structures", *Comput. Aid. Civil Infrastr. Eng.*, **9**(2), 119-128. https://doi.org/10.1111/j.1467-8667.1994.tb00367.x.

Tanoli, W.A., Naseer, A. and Wahab, F. (2014), "Effect of steel fibers on compressive and tensile strength of concrete", *Int. J. Adv. Struct. Geotech. Eng.*, **3**(4), 393-397.

Vairagade, V.S. and Kene, K.S. (2013), "Strength of normal concrete using metallic and synthetic fibers", *Procedia Eng.*, **51**, 132-140. https://doi.org/10.1016/j.proeng.2013.01.020.

Woo, S.K., Kim, K.J. and Han, S.H. (2014), "Tensile cracking constitutive model of Steel Fiber Reinforced Concrete (SFRC)", *KSCE J. Civil Eng.*, **18**(5), 1446-1454. https://doi.org/10.1007/s12205-014-0335-3.

Yazici, S., Inan, G. and Tabak, V. (2007), "Effect of aspect ratio and volume fraction of steel fiber on the mechanical properties of SFRC", *Constr. Build. Mater.*, **21**(6), 1250-125. https://doi.org/10.1016/j.conbuildmat.2006.05.025.

Yehia, S., Douba, A., Abdullahi, O. and Farrag, S. (2016), "Mechanical and durability evaluation of fiber-reinforced self-compacting concrete", *Constr. Build. Mater.*, **121**, 120-133. https://doi.org/10.1016/j.conbuildmat.2016.05.127.

Yi, T., Li, H. and Sun, H. (2013), "Multi-stage structural damage diagnosis method based on "energy-damage" theory", *Smart Struct. Syst.*, **12**(3-4), 345-361. https://doi.org/10.12989/sss.2013.12.3_4.345.

Yoo, D.Y., Banthia, N., Kang, S.T. and Yoon, Y.S. (2016), "Effect of fiber orientation on the rate-dependent flexural behavior of ultra-high-performance fiber-reinforced concrete", *Compos. Struct.*, **157**, 62-70. https://doi.org/10.1016/j.compstruct.2016.08.023.

Yoo, D.Y., Yoon, Y.S. and Banthia, N. (2015), "Flexural response of steel-fiber-reinforced concrete beams: Effects of strength, fiber content, and strain-rate", *Cement Concrete Compos.*, **64**, 84-92. https://doi.org/10.1016/j.cemconcomp.2015.10.001.

Zhang, Z.H., Liu, X., Zhang, Y., Zhou, M.L. and Chen, J.G. (2020), "Time interval of multiple crossings of the Wiener process and a fixed threshold in engineering", *Mech. Syst. Signal Pr.*, **135**, 106389. https://doi.org/10.1016/j.ymssp.2019.106389.

Zhang, Z.H., Zhou, M.L. and Fang, M. (2019), "First-passage probability analysis of Wiener process using different methods and its applications in the evaluation of structural durability degradation", *Eur. J. Environ. Civil Eng.*, 1-19. https://doi.org/10.1080/19648189.2019.1601134.

Ziolkowski, P. and Niedostatkiewicz, M. (2019), "Machine learning techniques in concrete mix design", *Mater.*, **12**(8), 1256. https://doi.org/10.3390/ma12081256.

CC